IAC-18-B4.8.11

Modeling of Orbital and Attitude Dynamics of Nanosatellites Controlled via Active Electrostatic Charging

Filippo Corradino[a]*, Marco B. Quadrelli[b], Sabrina Corpino[a]

[a] Politecnico di Torino, Department of Mechanical and Aerospace Engineering, Corso Duca degli Abruzzi 24, 10129 Torino, Italy

[b] Jet Propulsion Laboratory, California Institute of Technology, 4800 Oak Grove Drive, Pasadena, CA 91109-8099, U.S.A

*Corresponding author

Abstract

The large-scale exploration of airless bodies, such as asteroids and moons, is gaining interest, however it is limited by mobility issues: the lack of atmosphere, low gravity, and unknown soil properties pose difficult challenges for many forms of traditional locomotion. The environment in proximity of these bodies is also electrically charged due to interactions with solar wind and UV radiation. The EGlider (Electrostatic Glider) concept would be able to overcome these mobility issues by leveraging the natural environment, allowing operations in close proximity of the surface, while enabling long duration missions by minimizing propellant consumption. The EGlider is an advanced concept for small satellite mobility and propulsion, which relies on the electric fields naturally present around airless bodies in order to generate forces and torques useful for maneuvering. It does so by extending electrically charged appendages, which enable it to electrostatically soar above the surface. By differentially charging its electrodes it can also produce torques to control its attitude. The charges are maintained by continuous active ion or electron emission from the spacecraft, in order to cancel out the neutralizing influx of charges from surrounding plasma. An investigation of the spacecraft-plasma interaction was carried out. This included studying the effect of electrode geometry and calculating the charge-to-mass ratios required to enable several mission scenarios. Long, thin wire electrodes were identified to be the most power-efficient and would allow power-to-weight ratios achievable with current nanosatellite technologies. High electrode potential represents the main limiting factor for the system design. In order to test the feasibility of active control by means of differential charging, a simple 2D interaction model was developed, and a feedback controller to stabilize the vehicle was tested in a simulation environment. The results confirmed that good performance could be obtained for both position and attitude control. Finally, a dedicated software was developed for future simulation and testing of control strategies for the EGlider. This software allows to study the trajectory and attitude of an arbitrarily configured spacecraft in the proximity of an arbitrarily defined main airless body. The spacecraft can be assembled from basic parts, each with specified electrical, mass and optical properties. Efficient models allow to calculate gravitational and electrical interactions with the rotating main body and the local plasma field, as well as solar radiation pressure effects. Control models can be implemented as simple plug-in functions and easily tested. The preliminary validation campaign showed good matching with the reference cases that have been analyzed.

Keywords: dynamics, control, asteroid, electrostatics, micro-gravity, nanosatellite

Acronyms/Abbreviations

AU	Astronomical Unit
LVLH	Local Vertical Local Horizontal
RIC	Radial / In-Track / Cross-Track
S/C	Spacecraft
SRP	Solar Radiation Pressure
UV	Ultraviolet

1. Introduction

The large-scale exploration of airless bodies, such as asteroids (including NEAs, Near Earth Asteroids), moons, and comets, by means of small satellites, is becoming of great interest. NASA has been very active in this field [1], with the remarkable achievement of launching and operating MarCO, the first CubeSat to leave Earth orbit heading to Mars [2], and Lunar CubeSats as secondary payload on SLS/Orion EM-1 [3]. Among these, the Near-Earth Asteroid Scout 6U CubeSat (NEA Scout), developed jointly between NASA's Marshall Space Flight Center and the Jet Propulsion Laboratory, is a robotic reconnaissance mission that will be deployed to fly by and return data from an asteroid representative of NEAs that may one day be human destinations [4]. Recently, a number of studies have been made or planned related to interplanetary CubeSat missions at ESA, all supported by the General Studies Programme (GSP) [5]. These include the CubeSat Opportunity Payloads (COPINS) in the Asteroid Impact Mission at Didymos [6], and the LUnar CubeSats for Exploration (LUCE) [7] studies, all targeted at focussed scientific missions with compact instrumentation at

distances remote from Earth. They are based on mother-daughter architectures where the mother-craft transports the CubeSats to a target destination, deploys them locally to perform their mission, and provides data relay support back to Earth for TT&C and payload data downlink enabled by a bi-directional inter-satellite link. The Miniaturised Asteroid Remote Geophysical Observer (M-ARGO) CDF (Concurrent Design Facility) study proposed instead to develop a standalone platform, compatible with multiple objectives and targets [8]. Doing valuable science and/or supporting space exploration objectives in the vicinity of an asteroid poses a set of challenges for these tiny platforms in all areas of the mission, from technology to operations.

All proposed missions and studies highlight the issue of orbit maintenance during operations at the asteroid(s) and of fine attitude control required for science payloads and antenna pointing during the science mission phase [9]. Operating in a controllable manner close to these bodies surfaces is often limited by lack of knowledge, surface hazards, and mobility issues: the environment is challenging both for traditional orbiting spacecrafts (since, due to the very low gravity, stable orbits are hard to achieve) and for mobile landers with hopper or micro-gripper locomotion, which depend on having sufficient friction against the unknown surface to function [1,2]. The lack of an atmosphere finally prevents the use of aerodynamic flyers. All proposed missions and studies feature traditional Attitude Control Systems based on the combination of reaction wheels and control jets, while propulsion and orbit control functions are accomplished either by solar sails, or by electric or chemical (monopropellant) systems.

To enable these challenging NASA small body missions, this paper proposes the E-Glider concept [1,2], as an effective means to maneuver in proximity of the surface at low fuel cost.

The space environment in proximity of these bodies is electrically charged due to interactions with the solar wind plasma and UV radiation [3,4,5,6]. The E-Glider concept proposes to exploit these electric fields and the solar wind plasma naturally present around airless bodies in order to generate forces and torques for small satellite mobility, propulsion and attitude control. This can be accomplished by extending electrically charged appendages (or electrodes), which allow, for instance, to levitate over the similarly charged surface of an asteroid.

The E-Glider would extend strands of metallic film, to form distributed electrodes that interact with the local plasma. By articulating these electrodes, the E-Glider would also be able to not only translate, but also change its attitude, without touching the surface.

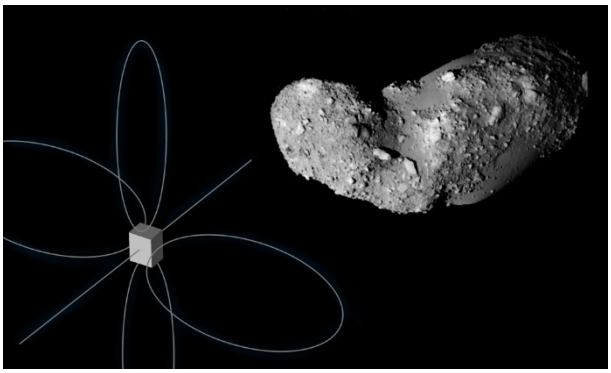

Fig. 1. Artist rendering of an E-Glider spacecraft in the proximity of Itokawa, sporting thin wire electrodes

The charges are maintained by continuous ion or electron emission (as necessary) from the spacecraft, by means of small ion guns or other techniques, in order to cancel out the neutralizing influx of charges from the surrounding plasma. The (electric) power expenditure needed to accomplish this function could virtually be the whole "cost" of the E-Glider propulsion system, thus enabling long duration missions without the issue of propellant consumption.

1.1 Objectives of this study

A substantial body of work was already available on the E-Glider concept [1,2]. The objective of the study presented in this paper was to build upon the existing work, with particular focus on three areas:

- Applying refined models to tackle the plasma physics and electrostatics of the E-Glider interaction with the electric environment, in particular to overcome the limitations of some excessively simplified analytical models used so far.
- Evaluating the feasibility of position/attitude control through active charging by demonstrating a simple control strategy through simulation (only passive equilibria were considered in previous studies), assuming that knowledge of the surrounding plasma conditions is available in real-time.
- Developing a complete orbital and attitude dynamics simulator, valid for arbitrary spacecraft geometries and main body properties, including modeling of gravitational, radiation pressure and electrostatic interaction, to be used for further and more detailed analyses.

The main assumptions underlying the research in this paper are as follows:

- Quiescent plasma environment, with typical Debye length between between 0.5 and 10 meters, and parameters shown in Table 1.
- Perfect knowledge of the surrounding plasma conditions is available in real-time.

- The spacecraft is a rigid body with rigid appendages.
- Keplerian or near-Keplerian orbital dynamics.
- Near spherical gravitational fields
- Non-spinning small body.
- Near perfectly specular surfaces.

1.1 Paper sectional organization

Section 2 of this paper is dedicated to the background information, assumptions and methodology of the work done, while Section 3 goes over the main results and their discussion. Conclusions and final remarks are presented in Section 4.

Sections 2 and 3 are themselves split in 4 parallel subsections, dealing with:

- The electrostatic environment of airless bodies, i.e. the general characteristics of the plasma and electric fields, as well as the dynamics of a charged spacecraft (2.1, 3.1).
- The feasibility of a position and attitude control based on active charging (2.2, 3.2).
- Plasma collection currents and power/potential generation requirements for an actively charged spacecraft in a plasma (2.3, 3.3).
- The development of the complete high-fidelity orbital and attitude dynamics simulator for use in follow-on work (2.4, 3.4).

2. Methodology and theory

2.1 Electrostatic environment and dynamics

2.1.1 Plasma and charge environment on airless bodies

Most asteroids (and, more generally, airless bodies) can be modeled as high-resistivity spheroidal bodies immersed in the solar wind plasma stream. The side facing the incoming solar wind is also illuminated by the Sun. Both the solar wind and the solar radiation interact with the surface to generate or exchange charges. [4,5].

At the representative distance of 1 AU the solar wind is composed of ions (mainly protons) and electrons, with the properties listed in Table 1:

Table 1. Solar wind and plasma parameters at 1 AU

Parameter		Value	
Ion density	n_i	$5 \cdot 10^6$	#/m3
Electron density	n_e	$5 \cdot 10^6$	#/m3
Ion temperature	T_i	10	eV
Electron temperature	T_e	15	eV
Debye length	λ_D	10	m
Drift speed	V_s	350	km/s
Mach number	M	10	

The solar wind at 1 AU is mesosonic: the ions are supersonic, i.e. their drift velocity is much greater than their thermal velocity, while the electrons are subsonic, since their lower mass and greater mobility mean they have much higher thermal velocities. For this reason, the ions streaming past the asteroid form a significant wake behind it, in which only the mobile electrons can penetrate. Only electrons can therefore impinge on the dark side of the body, which negatively charges until the local electric field is strong enough to reflect all incoming electrons. At equilibrium, the potential on the dark side can thus reach negative values of tens to several hundreds of volts.

On the sunlit side, UV radiation extracts photoelectrons with energies of 2 to 3 eV from the surface, thus inducing a small positive charge of a few volts with respect to the unperturbed equilibrium potential.

Due to the high resistivity, neutralizing currents within the celestial body are limited, and these local charges accumulated on the surface are mostly maintained; thus, high potential gradients can be present on the asteroid surface, especially at the terminator region, which lies in between the two differently charged hemispheres. [3,4,5,6]

A PIC (Particle-In_Cell) simulation of the plasma environment around a sample asteroid was recently performed by William Yu and prof. Joe Wang of USC [7]. The body considered was a 28 m diameter dielectric sphere at 1 AU from the Sun. The objective of this analysis was to obtain good resolution 3D data of species densities, electrostatic potential and field, in order to evaluate the charging requirements and plasma interaction of an E-Glider for a mission in this representative environment.

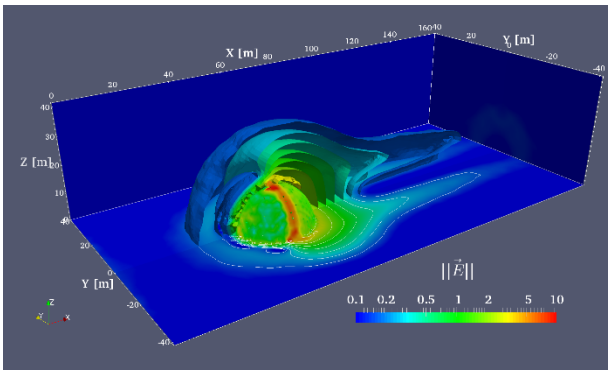

Fig. 2. Electric field magnitude around a small asteroid - PIC analysis courtesy of J. Wang and W. Yu of USC.

2.1.2 Electrostatic orbiting

The first objective of this work is to identify, at least qualitatively, the E-Glider charge-to-mass requirements for performing operations in proximity of the reference asteroid, in particular to maintain periodic trajectories around the body.

The main forces at play are:

- Gravitational attraction of the asteroid

- Electrostatic forces due to the plasma and surface-generated electric fields
- Solar radiation pressure
- Apparent forces in the non-inertial Hill frame of the asteroid-Sun two-body system.

The apparent forces are several orders of magnitude smaller than the others, and introduce periodic motions with long characteristic times of approximately 1 year, and could thus safely be neglected for this first approximation analysis.

The spheroidal asteroid model used shows a symmetry about the subsolar axis (i.e. the incoming direction of both solar wind and solar radiation). It is therefore assumed that all external fields acting on the spacecraft can be expressed as a function $f(X,R)$ of the coordinate along the subsolar axis (X) with origin at the asteroid center, and a radial coordinate (R) perpendicular to said axis. On the subsolar axis (X) itself, it can also be assumed that for any external field F its radial component F_R must be null.

Finding periodic trajectories which revolve around the (X) axis simply equates to finding equilibrium points in the (X; R) plane, also taking into account the radial apparent forces introduced by the revolution about the (X) axis. This equilibrium can be written as:

$$\frac{1}{m}\mathbf{g} + a_p\hat{\mathrm{X}} + \frac{Q}{m}\mathbf{E} + \frac{L_X}{R^3}\hat{\mathrm{R}} = 0 \qquad (1)$$

where $\mathbf{g}$ and $\mathbf{E}$ are respectively the gravitational acceleration and electric fields, while the spacecraft is characterized by a mass m, a charge Q, and an angular momentum L_X about the (X) axis, and $\hat{\mathrm{R}}$ is the radial unit vector. For the gravitational force a point-mass model is used, while for the Solar Radiation Pressure (SRP) a simple cannonball model is assumed and a constant acceleration a_p directed along X is imposed on the spacecraft (when this is not shadowed by the asteroid).

This 2D equation can be solved to find Q and L_X values for each point of the (X; R) plane. For any circular trajectory around the subsolar axis of given position and radius, one can therefore find a value of spacecraft charge to balance out forces in the (X) direction, while the forces in the radial (R) direction are balanced out with the added contribution of the centrifugal effect of an appropriate tangential velocity (Fig. 3).

This kind of E-Glider trajectories are given the name of "electrostatic orbits".

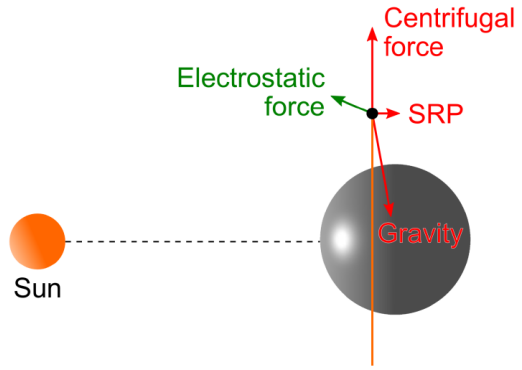

Fig. 3. Electrostatic orbiting forces diagram

A special case of electrostatic orbits of particular interest is represented by those for which the radial coordinate is null, i.e. the E-Glider lies on the subsolar axis; in this case it is perhaps more adequate to talk about "electrostatic hovering", since basically the E-Glider is hovering above the surface, stationary with respect to the subsolar point (Fig. 4).

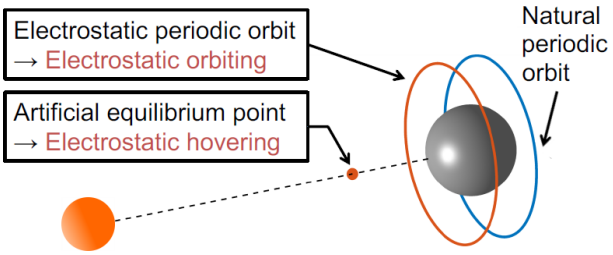

Fig. 4. Illustration of subsolar hovering and both passive and active terminator orbiting trajectories, from [15].

2.2 Active charge control

One of the key features of the E-Glider concept is the ability to perform both orbit/trajectory control and attitude control with the same (and virtually propellant-less) method of charge control. Net and differential surface charging enables the E-Glider to generate forces and torques not only to maintain static equilibrium, as illustrated in the previous paragraph, but also to contrast disturbances and actively modify its trajectory or attitude to navigate around an airless body.

The goal of the research is to demonstrate the general feasibility of such an approach for position and attitude control through net and differential charging. A key assumption is that knowledge of the surrounding plasma conditions is available to the E-Glider in real-time. Details of the sensing approach of the plasma conditions are outside the scope of this paper. To this end, a small set of simulations has been performed on a simple analytic E-Glider dynamics model, presented in the following paragraphs.

2.2.1 Control system model

The same simplified 2D cylindrical coordinates model used in section *2.1* is adopted to describe the environment in which the E-Glider operates. A simple 2D spacecraft model is used for the E-Glider itself (Fig. 5), with four symmetrical electrodes around a central rigid bus, aligned to a set of body axes (x; y).

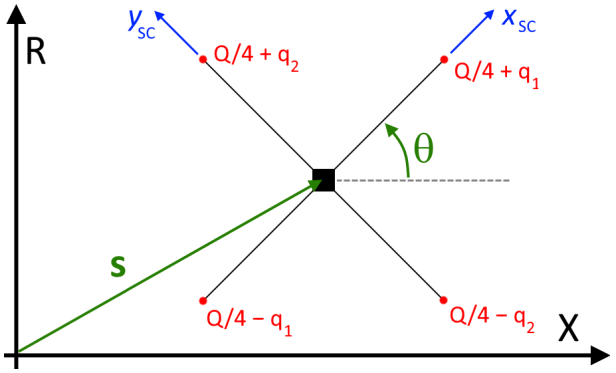

Fig. 5. Reference frame and control variables for the active control analysis

The charge was only localized at the tip of the four rigid appendages, each with length $b/2$, and charge distribution can be described by three variables:

- Q, the "common mode" net spacecraft charge, equally distributed on the four electrodes.
- q_1, the first "differential mode" charge, on the x axis electrode pair: $+q_1$ on the electrode with positive x coordinate and $-q_1$ on the electrode with negative x coordinate.
- q_2, the second "differential mode" charge, on the y axis electrode pair: $+q_2$ on the electrode with positive y coordinate and q_2 on the electrode with negative y coordinate.

The position of the spacecraft is $\mathbf{s}$, while θ represents the angle between the spacecraft x axis and the global X axis: $\mathbf{s}$ and θ are the state variables.

The controller receives a certain commanded reference state ($\mathbf{s}_0$; θ_0) and acts based on the error between this and the current state. A simple PID (Proportional, Integral, Derivative) controller is used for this purpose, and translates the error in desired accelerations along the three state axes ($\ddot{\mathbf{s}}$; $\ddot{\theta}$). These acceleration commands are then translated with a custom fitting model into the actual control charges variables, i.e. (Q; q_1; q_2). Finally, the system responds to the control variables following the dynamics equations.

Fig. 6 illustrates the control system in block diagram form.

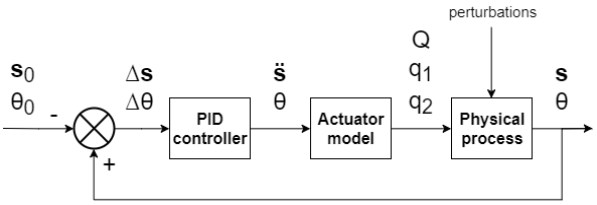

Fig. 6. Block diagram of the active control system

2.2.2 System dynamics

Extending Eq. (1) to the reference spacecraft geometry, including also rotation in the (X; R) plane, can be shown to yield the following [8]:

$$\begin{cases} \ddot{\mathbf{s}} = \frac{1}{m}\mathbf{g}(\mathbf{s}) + a_p\hat{\mathrm{X}} + \frac{Q}{m}\mathbf{E}(\mathbf{s}) + \mathbf{G}_e(\mathbf{s})\frac{\mathbf{S}_q}{m} + \frac{L_X}{R^3}\hat{\mathrm{R}} \\ \ddot{\theta} = \frac{1}{I_{mz}}\left(\mathbf{S}_q \times \mathbf{E}(\mathbf{s})\right)\cdot\left(\hat{X}\times\hat{R}\right) \end{cases} \quad (2)$$

Where I_{mz} is the rotational inertia of the spacecraft in the (X; R) plane, $\mathbf{G}_e$ is the electric field gradient tensor, and $\mathbf{S}_q$ is the first moment of charge of the spacecraft, i.e its electric dipole. This dynamics model corresponds to the "Physical process" block in Fig. 6. It is assumed that the angular momentum L_X can be independently controlled (it is indeed controlled by forces external to the (X; R) plane considered here), therefore its value was set to the equilibrium value at $\mathbf{s}_0$ obtained from Eq. (1).

2.2.3 Actuation law

A model to translate commanded accelerations into control charges is also required (the "Actuator model" block in Fig. 6). Assuming that $\mathbf{s}\sim\mathbf{s}_0$, one can rewrite Eq. (2) to isolate a static equilibrium part and a dynamic control part; Q can be written as Q_0+dQ, where Q_0 is the equilibrium net charge at $\mathbf{s}_0$ obtained from Eq. (1).

Therefore, for small perturbations:

$$\begin{cases} \ddot{\mathbf{s}} = \frac{dQ}{m}\mathbf{E}(\mathbf{s}) + \mathbf{G}_e(\mathbf{s})\frac{\mathbf{S}_q}{m} \\ \ddot{\theta} = \frac{1}{I_{mz}}\left(\mathbf{S}_q \times \mathbf{E}(\mathbf{s})\right)\cdot\left(\hat{\mathrm{X}}\times\hat{\mathrm{R}}\right) \end{cases} \quad (3)$$

dQ and $\mathbf{S}_q$ can then trivially be translated into (Q; q_1; q_2) by means of a simple function of the S/C rotation θ and Q_0. This way one can directly relate a commanded accelerations vector to the control charges vector. This law actually presents a singularity on the X axis, since on it the radial position cannot be controlled (E_R = G_{eXR} = G_{eRX} = G_{eRR} = 0); a deadband is therefore prescribed close to the axis and a dedicated simplified actuation law is used while inside of it.

2.2.4 PID controller

The final component of the control system is the controller, which commands the required accelerations given the state vector error. The controller is composed

of three parallel PIDs which act independently on each axis. A combination of the Ziegler-Nichols method and trial and error was employed to obtain a preliminary tuning of the PIDs.

The integral component is only applied on the *X* axis, the other controllers are more properly PDs. An anti-windup saturation limit was imposed on the integral component, and saturation limits were imposed on the electrode charge values.

2.3 Plasma/Spacecraft interaction

Another issue of interest when evaluating the feasibility of an E-Glider concept, concerns the power and electrostatic potential constraints.

Any electrically biased object immersed in a plasma will be subject to a current from the plasma which tends to bring it to an equilibrium potential. Since the E-Glider must maintain and control its charge state, the return currents must be actively and precisely re-emitted. Since the emitted charges must have at least sufficient energy to escape the potential well off the spacecraft, a good indicator of the power needed for charge-keeping is the product of collected current and electrode voltage.

A range of current collection analyses have been carried out to study this effect, assuming different electrode geometries, charge-to-mass ratios, and plasma conditions.

2.3.1 Electrode voltage

The electrode voltage depends on its charge and capacitance, and the capacitance in a plasma depends on both the electrode dimensions and the local sheath thickness (a thin sheath boosts the capacitance). The sheath thickness however depends on the electrode voltage itself as shown by Eq.(4). An iterative process is therefore usually required in order to find the correct electrode voltage.

$$\begin{aligned} C &= C(\lambda_D) = C(V) \\ V &= V(Q, C) \end{aligned} \tag{4}$$

where λ_D is the plasma Debye length. The capacitance in a vacuum can be assumed as a tentative value to obtain an initial conservative estimate of the bias voltage V_0. Equations (4) can then be iterated until convergence.

2.3.2 Collection currents

There are several empirical and analytical models for collection currents to electrodes of various shapes available in literature [9,10,11]. These were specifically applied to evaluate currents and potentials for spherical, cuboidal, or thin wire (both straight or looped) electrodes, using typical charge-to-mass ratios inferred from the analyses presented in sections *2.1* and *2.2*, in order to identify the pros and cons of each shape for an E-Glider application.

2.3 Simulation

A spacecraft dynamics simulator was developed in Python, with the objective of performing accurate trajectory and attitude simulations of an arbitrarily defined simple spacecraft in the proximity of an arbitrarily defined main body. These spacecrafts and main bodies can be defined step-by-step with the help of dedicated Constructor Scripts, and then saved to file. This allows to decouple the simulation objects definition from the simulation itself.

- Spacecraft of different configurations can be defined through the addition of "parts", in a similar fashion to many multibody codes. Each part is based on a simple reference geometry, such as sphere, cuboid, plate or cylinder. For each part, any one or more among geometry, mass, electrical and SRP properties can be defined in detail.
- Main Bodies are defined through parameters such as mass, geometry, gravity model (e.g. spherical harmonics), rotational and orbital parameters, and local plasma field data. The orbital parameters can also be obtained from the JPL Small Bodies Database [12], while the plasma data can be directly read from PIC simulations output, by means of specially formatted text files.

The main simulator itself allows to propagate trajectory and attitude of a selected spacecraft in proximity of a selected main body. Control models can be implemented as simple plug-in functions to the main integrator and easily tested.

The simulator was named AMOSPy, for Airless-body Multifield Orbital Simulator in Python. The "Multifield" attribute is to signify that the simulator is suited to model not only gravitational, but also electrical, solar radiation pressure, or drag interactions, as desired for each analysis, for both trajectory and attitude propagation. The following paragraphs will elaborate on the force models available in AMOSPy.

2.4.1 Force fields

A first category of force models are those based on a vector field, such as the gravitational or electrostatic force. The vector field values can be derived either analytically (e.g. spherical harmonics gravity) or numerically (e.g. interpolation of PIC data for the electric field); in any case, both a field vector and a field gradient tensor can be obtained for any given point in space.

These fields act on a quantity, such as mass or charge, which is distributed over the whole spacecraft extended body, and thus generate both forces and torques. AMOSPy allows to calculate these in two ways [8]:

- With a linearized model, by using the net distributed quantity and its moments (e.g. total

mass and inertia), globally calculated from the ones of all the spacecraft parts, and using a single local value of field and field gradient.
- With a multipart model, by treating all parts as point-like and calculating the applied force due to the field at that precise point. The global force and torque are calculated from these forces applied on each point-like part.

2.4.2 – Surface interactions

Another category of interactions are those that can be modeled by momentum exchanges on the exposed surfaces, such as SRP or aerodynamic drag. Simple analytical methods can be used, such as the "cannonball model", however most are overly simplified and often don't even provide torque estimation. More accurate models are required when dealing with spacecrafts such as an E-Glider, with its large and lightweight electrode surfaces.

AMOSPy implements a simple ray-tracing model to estimate the effect of incident photons or particles. Each surface part of the spacecraft can be assigned values of absorptivity and specular/diffuse reflectivity; the surface is then meshed with a large number of small plane "facets", and a ray is generated on each one, to calculate a local elementary force contribution. Ray-tracing intersection algorithms then filter out the contributions from rays which would have been shadowed by other surfaces. This method guarantees that all surfaces are represented and sampled equally, as opposed to generating a bundle of external rays and casting them towards the spacecraft (forward ray-tracing), which can induce significant aliasing and gross errors when dealing with very thin features. Precision can be arbitrarily increased by using denser meshes.

While certainly possible for slow enough dynamics, it is generally still impractical to perform these computations in real-time in every scenario without a significant loss of precision. Therefore, forces and torques are all pre-calculated in a number of points over a map of possible attitudes, and then interpolated as necessary during the real-time integration and corrected with the actual local photon or particle flux.

2.4.3 Core dynamics

Finally, the external forces applied on the spacecraft need to be integrated into a set of equations of motion. AMOSPy develops the spacecraft dynamics in the RIC (or Hill, or LVLH) reference frame of the main body [14], supposed to be on a heliocentric keplerian orbit.

If the eccentricity of this orbit is low enough, the simple linear model of Clohessy-Wiltshire equations can be used effectively. However, airless bodies orbiting the Sun often are not on quasi-circular orbits, therefore AMOSPy is also equipped with a modified version of the CW system which is valid for elliptical orbits; this approximates the local orbital motion of the main body up to the second order (assumes constant angular acceleration, or zero jerk). The velocity (v_r, v_i, v_c) and position (r_r, r_i, r_c) state vector time derivative can be shown to be as follows, in state-space matrix form and in the RIC reference frame [8]:

$$\frac{d}{dt}\begin{Bmatrix} v_r \\ v_i \\ v_c \\ r_r \\ r_i \\ r_c \end{Bmatrix} = \left[A\left(\nu(t)\right)\right]\begin{Bmatrix} v_r \\ v_i \\ v_c \\ r_r \\ r_i \\ r_c \end{Bmatrix} + \begin{Bmatrix} f_r \\ f_i \\ f_c \\ 0 \\ 0 \\ 0 \end{Bmatrix} \tag{5}$$

$$[A] = \begin{bmatrix} 0 & 2\dot{\nu} & 0 & \frac{\mu}{2d^3} + \dot{\nu}^2 & -\dot{\nu} & 0 \\ -2\dot{\nu} & 0 & 0 & \dot{\nu} & -\frac{\mu}{d^3} + \dot{\nu}^2 & 0 \\ 0 & 0 & 0 & 0 & 0 & -\frac{\mu}{d^3} \\ 1 & 0 & 0 & 0 & 0 & 0 \\ 0 & 1 & 0 & 0 & 0 & 0 \\ 0 & 0 & 1 & 0 & 0 & 0 \end{bmatrix}$$

Electrostatic and gravitational interactions with the main body, as well as SRP and drag forces, can be simply added in the control vector. The state matrix is time-dependent and relies on a single dynamic parameter, which is $\nu(t)$, the true anomaly of the main body on its heliocentric orbit (the other terms, μ and d, are respectively the Sun gravitational parameter and the Sun-asteroid distance, of which μ is constant and d directly depends on ν). A very fast keplerian solver was implemented to calculate $\nu(t)$ [13]. The spacecraft attitude is parameterized with a classic quaternion-based system with respect to the inertial frame.

3. Results and Discussion

3.1 Electrostatic environment and dynamics

The plot in Figure 7 shows the axial electric field and the required charge-to-mass ratio required to perform electrostatic orbiting, in proximity of a 28 m asteroid at 1 AU from the Sun. A spacecraft surface-to-mass ratio of 0.1 m^2/kg was assumed, as well as an asteroid uniform density of 2200 kg/m^3 to compute the gravitational acceleration.

The deep blue arc extending from behind the terminator and up to the asteroid shadow traces the locus of passive SRP/gravity equilibrium. An object on this line would be able to orbit the asteroid even with no charge, perhaps using charge control simply as a means of stationkeeping and control against external perturbations (as shown in *2.2*). These trajectories are called terminator orbits [14]. One disadvantage of these trajectories, however, is that they are offset on the dark side of the asteroid, and thus offer low coverage in the illuminated side for visible spectrum optical payloads.

In proximity of the terminator region, where the electric field is strongest, the charge-to-mass required for electrostatic orbiting is however in the range of -1 μC/kg. A moderate spacecraft charge would therefore allow to "push" these passive terminator orbits towards the sunlit side, and thus greatly increase the coverage of illuminated areas on the surface (albeit still at low illumination angles).

Concerning instead hovering on the subsolar axis, the charge-to-mass ratios required are in the ballpark of -1 μC/kg over the dark side and -10 μC/kg over the sunlit side. Even though the charge required over the sunlit side is higher, from this vantage point the surface can be observed under constant illumination conditions, while the asteroid rotation slowly brings new parts of the surface into view under the E-Glider. Hovering over the dark side is very power-efficient, since not only the charge required is low, but the plasma is very rarefied, and there are almost no positive ions to form the return current, however no illumination prevents inspection of the asteroid surface in the visible spectrum, as well as solar power generation.

3.2 Active charge control

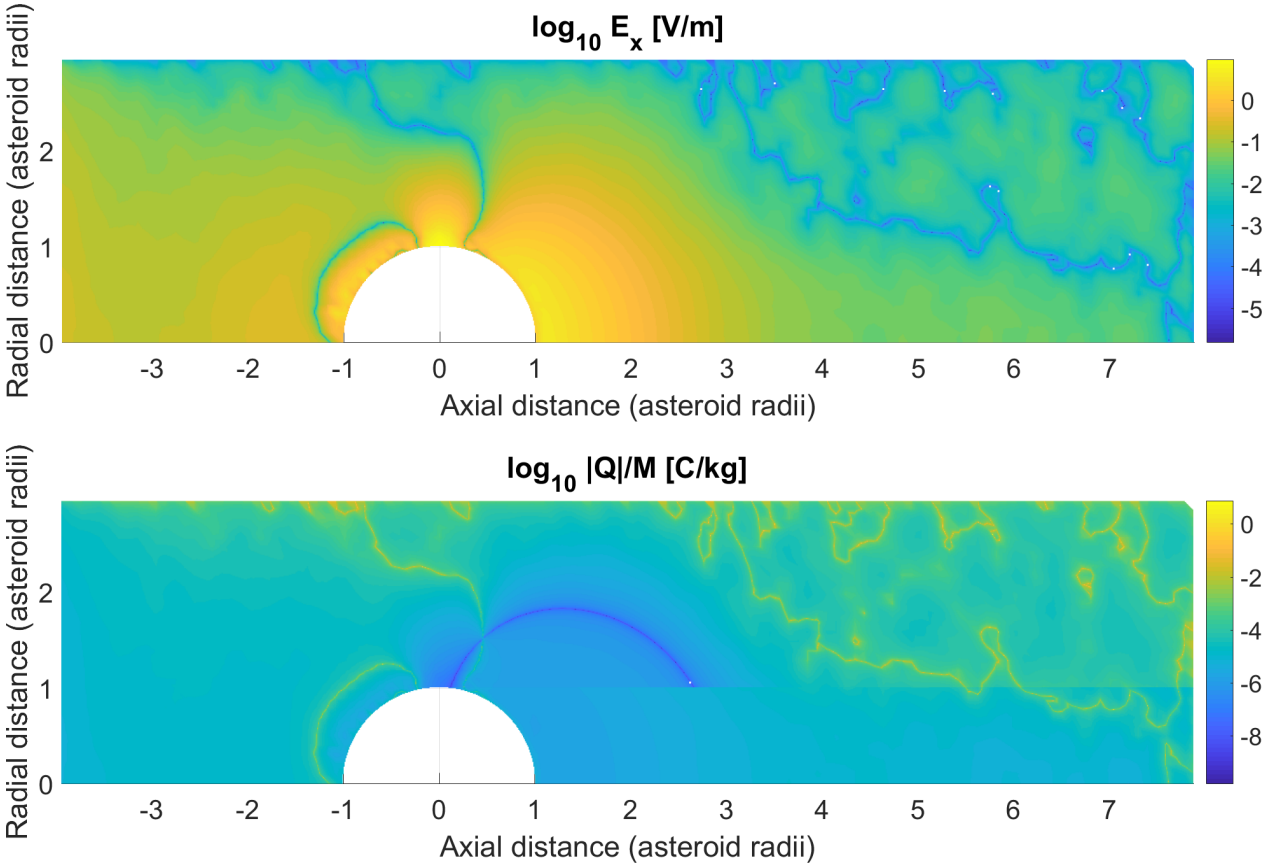

Fig. 7. Axial electric field (above) and charge-to-mass ratio (below) required for electrostatic orbiting

Even with a raw PID controller tuning, the results indicated that it is indeed possible to control both position and attitude by means of active charge control.

Fig. 8 displays the response of the system to a starting condition severely offset from equilibrium. The system converges to equilibrium with few to no oscillations along every axis. The net charge required for the control, apart from some initial saturation spikes, is never too far from the equilibrium values, therefore the increase in power consumption for this kind of active operation can be considered negligible or anyway manageable, especially if the errors are kept small and the controller remains far from saturation (such as in a stationkeeping or slow slewing situation).

Future work in this area would concern the expansion of the current model to a full 6-DOF control (three translations, three rotations), and testing of the expanded control algorithms in AMOSPy (*2.4*), which is well equipped to support this kind of controller.

It must be noted that in order to control the full 6-DOF state, since the system is underactuated, another electrode pair perpendicular to the first two would not be sufficient, since it would only introduce one new control in spite of three new axes to be controlled. Some other kind of pluri-electrode geometry, possibly with at least 5 or 6 electrode pairs should be implemented, in order to leverage not only the net charge Q and first moment of charge $\mathbf{S}_q$, but also the second moment of charge $\mathbf{I}_q$.

3.3 Collected currents

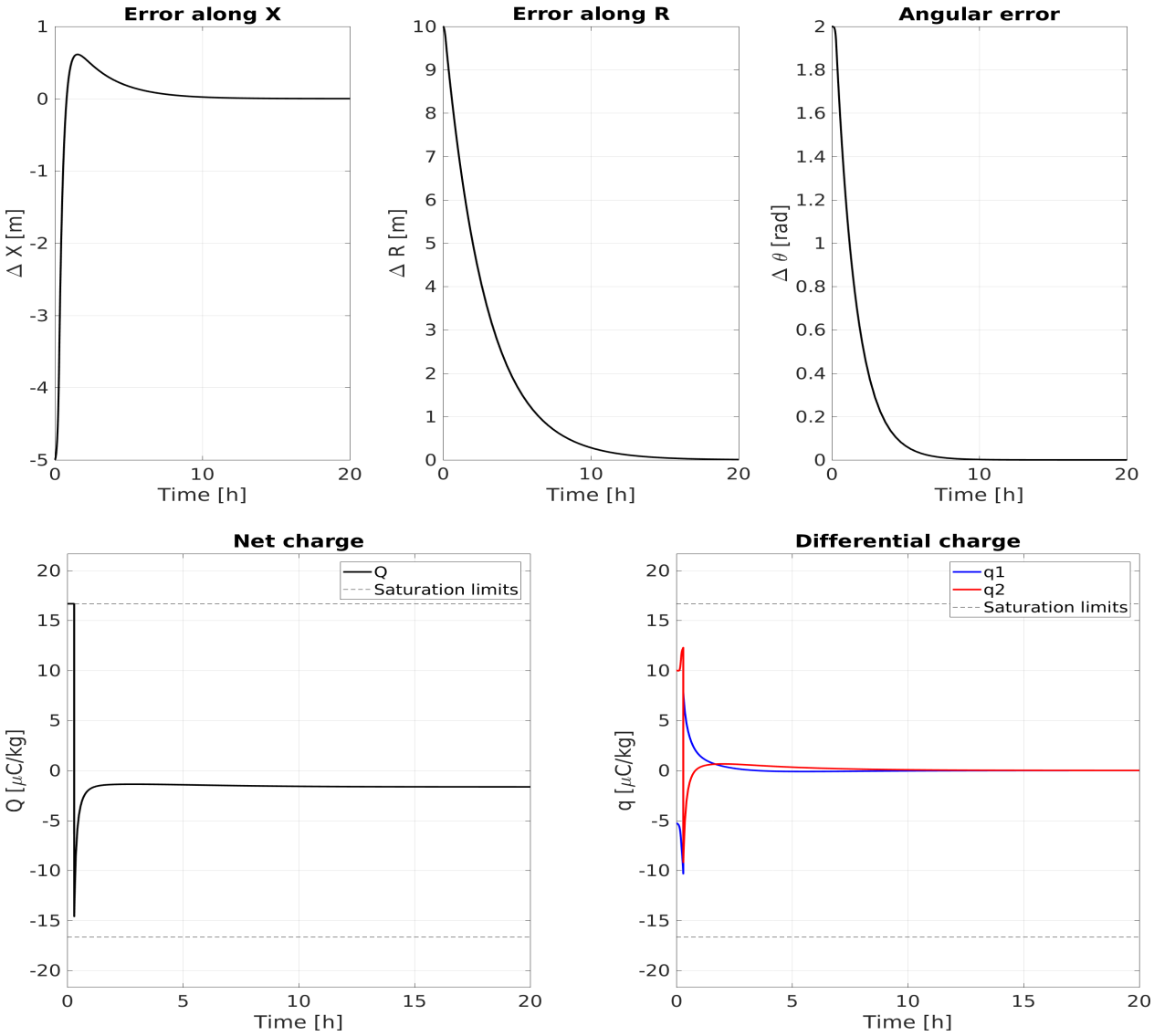

Fig. 8. Time-history of active control errors and controls in a terminator orbiting scenario

Previous work on the E-Glider [1][2] had focused primarily on spherical electrodes. Both spherical and cuboidal electrodes behaviour were evaluated in the context of this work, according to the models recently

developed by I. Bell [9]. The general advantage of these kind of electrodes is their high capacitance, which allows for reduced potentials. Low potentials are very desirable, since they imply lower return currents (and thus lower power), as well as less secondary parasitic effects such as sputtering, secondary electron and radiation emissions, and heating. On the other hand, a big drawback of these electrodes is their high surface area, and therefore their high current collection and often prohibitive power consumption.

Mitigation options for this issue were identified and could consist in using a relatively high number of electrodes with a certain optimal dimension. Spreading the charge over more than one electrode reduces the required potential, while increasing the collection area, but the first effect tends to dominate, thus using multiple electrodes can turn out to be convenient. Even with optimal conditions, however, the required power for subsolar hovering with these kind of electrodes turns out to be in the order of $10^2 \div 10^4$ W/kg [8], which is still impractical.

Wire electrodes were then evaluated. These electrodes are assumed to be lines or loops of thin wire, the radius of which is much smaller than one Debye length, thus the OML (Orbital Motion Limited) current collection theory was adopted. This theory shows very good accuracy in this thick-sheath regime [10,11].

These electrodes have opposite pros and cons with respect to the spherical/cuboid ones: while they have very little surface area (and therefore current collection), their capacitance is relatively low, and they require higher potentials.

The reduction in power consumption is however proportionally much more significant, and assuming that the necessary potentials can be achieved, this can easily bring the system power budget in the nanosatellite range of feasibility: $10^{-1} \div 10^0$ W/kg values can be achieved in hovering (more than 3 orders of magnitude decrease in power with respect to spherical electrodes) [8].

The limiting factor for a practical design would be the required potential. This is mostly influenced by the electrode length, and in the test case of a 3 kg E-Glider in subsolar hovering, more than 50 m of equivalent length would be needed if the potential is to be kept below 100 kV. This would be bulky but not unachievable, especially if multiple loop electrodes are arranged all around the spacecraft (e.g. 8 loops 2 m in diameter could be enough) [8].

Overall, thin wire electrodes seem to constitute a very promising option, especially in terms of power consumption, enabling the E-Glider concept to be applied to self-sufficient solar electric powered nanosatellites.

3.4 Simulation

AMOSPy has successfully undergone a series of tests to verify its correct working as well as its accuracy. Some analytical results have been compared to previous analyses and have been found to be in very good matching, with relative errors well below 1% [8].

Other interesting benchmarks that were performed include:

- Demonstration of the intermediate axis instability (Dzhanibekov effect [16]) to verify the attitude propagation models.
- Recreation of the passive stabilization of the Kepler Space Telescope with solar radiation pressure, to validate SRP force modeling. A simple spacecraft model was assembled, recreating the geometry of the solar arrays, main tube and S/C bus. A control law was implemented, in which two axes are actively stabilized by ideal reaction wheels, and the third is passively stabilized thanks to natural SRP torque on the solar array panels. The attitude propagation was indeed verified to be stable in the correct K2 prescribed attitude, and instable otherwise.

4. Conclusions

All three objectives set for this work (*1.1*) were reached with satisfactory conclusions.

Perhaps the most important result concerning the electrostatic interactions is the greatly reduced power requirement (when compared to the previous analyses [1,2]) obtained by employing thin wire electrodes, which brings the E-Glider concept into the feasibility range of power-to-weight ratio even for solar powered nanosatellites. Excessive electrode potentials are now probably the main limiting factor for the system design, and determining more precisely the feasibility limits for these (taking into account all kinds of secondary aspects, such as sputtering, secondary emission, thermionic emission, hard radiation, vacuum discharge...) will be useful in the future for determining more precisely the specific design constraints.

As for the active control dynamics, the results obtained in the simple 2D model are greatly encouraging and suggest that an extension to the full 3D model may very well be achievable. This could be a task for the future activities on the E-Glider dynamics modeling.

Assuming that knowledge of the surrounding plasma conditions is available in real-time, this result also proves the applicability of the E-Glider technology as a precision attitude control and stationkeeping system. Should it turn out that the requirements for the use of the E-Glider technology as a main propulsion system (hovering, levitation, ...) were impractical or unfeasible, it could still easily be repurposed as a precision manoeuvering or attitude control system. Moreover, this kind of application could perhaps be performed in a wider variety of environmental conditions. If the required forces/torques were limited, even the use in LEO could perhaps be feasible (e.g. as an intermediate solution

between magnetorquers and reaction wheels, with modest torques and no saturation).

Some investigations into application of the E-Glider in different environments in the Solar System, outside of the scope of this paper, have also been conducted, and interesting results have been obtained, even for applications in other planetary atmospheres.

Lastly, the multifield simulator AMOSPy has all the necessary capabilities for becoming in the future a valid software testbench for E-Glider concepts, and can allow the verification of active charge control algorithms, or trajectory stability analysis, or the calculation of power requirements for different plasma charging conditions. It can also easily be applied to study all kinds of other deep-space small satellites mission requiring similar conditions to the E-Glider. The main strong points of this simulator consist in enabling fast, nonsingular gravity models, a very accurate and robust ray-tracing algorithm to calculate solar radiation pressure effects, and a proximity dynamics model which is valid also for eccentric orbits of the target body.

Acknowledgements

U.S. Government sponsorship acknowledged. This research was carried out at the Jet Propulsion Laboratory, California Institute of Technology, under a NIAC Phase I-15-NIAC16B-0027 contract with the National Aeronautics and Space Administration under the NASA Innovative Advanced Concepts Program, and carried out at the Jet Propulsion Laboratory, California Institute of Technology, during a JVSRP (JPL Visiting Student Research Program) internship.

The authors would like to thank professor Joseph Wang and Dr. William Yu, from the University of Southern California, for valuable suggestions and for providing PIC data that was used in the analyses.

References

[1] M.B. Quadrelli et alii, NIAC Phase I Final Report - E-Glider: active electrostatic flight for airless body exploration, 2017

[2] M.B. Quadrelli et alii, Active electrostatic flight for airless bodies, 2017 IEEE Aerospace Conference, Big Sky, MT, 2017

[3] C.M. Hartzell, Dynamics of levitating dust particles near asteroids and the Moon, J. Geophys. Res. Planets 118, 2013

[4] P. Lee, Dust Levitation on Asteroids, Icarus 124, 0197, 1996

[5] D.A. Mendis et alii, On the Electrostatic Charging of the Cometary Nucleus, The Astrophysical Journal 249, 1981

[6] T. Nitter et alii, Levitation and dynamics of charged dust in the photoelectron sheath above surfaces in space, J. Geophys. Res. 103, A4, 1998

[7] J. Wang, W. Yu, University of Southern California, Private Communication

[8] F. Corradino, Master Thesis - Modeling of orbital and attitude dynamics of a satellite controlled via active electrostatic charging, Politecnico di Torino, 2018

[9] I.C. Bell III et alii, Experimental Investigation of Electron Collection by Rectangular Cuboid Probes in a High-Speed Plasma, IEEE Transactions on Plasma Science 45 7, 2017

[10] E. Choiniere et alii, Measurement of Cross-Section Geometry Effects on Electron Collection to Long Probes in Mesosonic Flowing Plasmas, 39th Joint Propulsion Conference and Exhibit, Huntsville, AL, 2003

[11] K.R.P. Furhop, Theory and Experimental Evaluation of Electrodynamic Tether Systems and Related Technologies, University of Michigan, 2007

[12] JPL Small-Body Database Search Engine, https://ssd.jpl.nasa.gov/sbdb_query.cgi, (accessed 10.09.18).

[13] M.A. Murison, A Practical Method for Solving the Kepler Equation, U.S. Naval Observatory, 2006

[14] D.J. Scheeres, Orbit mechanics about small asteroids, 20th International Symposium on Space Flight Dynamics, Annapolis, ME, 2007.

[15] S. Kikuchi, Coupled Orbit-Attitude Dynamics of Spacecraft around Small Celestial Bodies, PhD Thesis, Univ. of Tokyo, 2018.

[16] Hughes, P.C.: Spacecraft Attitude Dynamics, Wiley, 1986.